New Polylactide/Layered Silicate Nanocomposites. 1. Preparation, Characterization, and Properties

ARTICLE *in* MACROMOLECULES · APRIL 2002

Impact Factor: 5.8 · DOI: 10.1021/ma011613e

5 AUTHORS, INCLUDING:

Suprakas Sinha Ray
Council for Scientific and Industrial Research…
313 PUBLICATIONS **10,746** CITATIONS
SEE PROFILE

Pralay Maiti
Indian Institute of Technology (Banaras Hind…
102 PUBLICATIONS **3,640** CITATIONS
SEE PROFILE

Masami Okamoto
Toyota Technological Institute
124 PUBLICATIONS **10,976** CITATIONS
SEE PROFILE

New Polylactide/Layered Silicate Nanocomposites. 1. Preparation, Characterization, and Properties

Suprakas Sinha Ray,[†] Pralay Maiti,[†] Masami Okamoto,*[,†] Kazunobu Yamada,[‡] and Kazue Ueda[‡]

Advanced Polymeric Materials Engineering, Graduate School of Engineering, Toyota Technological Institute, Hisakata 2-12-1, Tempaku, Nagoya 468-8511, Japan, and Unitika Ltd., Kozakura 23, Uji, Kyoto 611-0021, Japan

Received September 10, 2001; Revised Manuscript Received January 15, 2002

ABSTRACT: New polylactide (PLA)/layered silicate nanocomposites have been prepared successfully by simple melt extrusion of PLA and organically modified montmorillonite. The *d* spacings of both the organically modified montmorillonite and intercalated nanocomposites were investigated by wide-angle X-ray diffraction (WAXD) analysis, and the morphology of these nanocomposites was examined by transmission electron microscopy (TEM). Using oligo(ϵ-caprolactone) (o-PCL) as a compatibilizer, the effect of compatibilizer in nanocomposites was investigated by focusing on two major aspects: morphological analysis and mechanical property measurements. The intercalated nanocomposites exhibited remarkable improvement of materials properties in both solid and melt states as compared to that of PLA matrices without clay.

Introduction

In recent years, polymer/layered silicate nanocomposites have received significant research attention, because they often exhibit remarkable improvement of mechanical, thermal, optical, and physicochemical properties when compared with the pure polymer or conventional composites (micro- and macrocomposites).[1−7] These improvements can include high moduli, increased strength and heat resistance, and decreased gas permeability and flammability.

With organically modified layered silicates (OMLS), nanocomposites have been produced from a broad spectrum of polymers with varying degrees of polarity and the chain rigidity such as polystyrene, poly(vinylpyridene), poly(ethylene oxide), poly(methyl methacrylates), polysiloxanes, polyphosphazenes, and main-chain liquid crystalline polymers.[5,8] Whether an admixture of polymer and OMLS produces an exfoliated or intercalated nanocomposites depends critically upon the characteristics of the polymer matrix and the OMLS. These characteristics include the nature of the polymer as well as the type, packing density, and the size of the organic modifiers on the silicate surface. One successful method to prepare polymer/layered silicate nanocomposites is to intercalate polymers into the silicate galleries. Generally, intercalation of polymer chains into silicate galleries is done by using one of the following two approaches: (1) insertion of suitable monomers in the silicate galleries and subsequent polymerization[9] or (2) direct insertion of polymer chains into the silicate galleries from either solution[10] or the melt.[11]

Since the possibility of direct melt intercalation was first demonstrated by Vaia et al.,[11] recently the melt intercalation method has become a main stream for the preparation of intercalated polymer/layered silicate nanocomposites because it is quite suitable for industrial uses.[12,13] This process involves annealing, statically or under shear, a mixture of the polymer and OMLS above the softening point of the polymer.[8] During the anneal, the polymer chains diffuse from the bulk polymer melt into the galleries between the silicate layers. Depending on the degree of penetration of the matrix into the OMLS galleries, nanocomposites are obtained with structures ranging from *intercalated* to *exfoliate*. Polymer penetration resulting in finite expansion of the silicate layers produces intercalated nanocomposites consisting of well-ordered multilayers with alternating polymer/silicate layers and a repeat distance of few nanometers.[14] On the other hand, extensive polymer penetration resulting in disordered and eventual delamination of the silicate layers produces exfoliated nanocomposites consisting of individual silicate layers dispersed in polymer matrix.[4]

Recently, PLA has received much research attention as of biodegradable polymers.[15−17] PLA is a linear aliphatic thermoplastic polyester, produced from renewable resources with excellent properties comparable to many petroleum-based plastics and readily biodegradable.[18,19] PLAs are produced either by ring-opening polymerization of lactides or by condensation polymerization of the lactic acid monomers, and these monomer are obtained from the fermentation of sugar feedstocks, corn, etc.[20] Generally, commercial PLA grades are copolymers of poly(L-lactide) and poly(DL-lactide). The amount of D-enantiomers is known to affect the properties of PLA, such as the melting temperature and the degree of crystallinity. PLA has high mechanical properties, thermal plasticity, fabric ability, and biocompatibility. It has been proposed as a renewable and degradable plastic for uses in service ware, grocery, waste-composting bags, mulch films, controlled release matrices for fertilizers, pesticides, and herbicides.[21] PLA possesses a relatively high melting temperature in comparison with other biodegradable aliphatic polyester such as poly(ϵ-caprolactone) (PCL), poly(butylene succinate) (PBS), etc. Accordingly, we have planned to design environmentally benign nanocomposites based

[†] Toyota Technological Institute.
[‡] Unitika Ltd.
* Corresponding author: tel +81-52-809-1861; fax +81-52-809-1864; e-mail okamoto@toyota-ti.ac.jp.

10.1021/ma011613e CCC: $22.00
Published on Web 03/09/2002

Table 1. Composition and Characteristic Parameters of Various PLACNs Based on PLA, o-PCL, and C_{18}-mmt

	composition, wt %							
sample	PLA	o-PCL	C_{18}-mmt[b]	$M_w \times 10^{-3}$ (g/mol)	M_w/M_n	T_g/°C	T_m/°C	χ_c[c]/%
PLACN1	97		3 [2.0]	178	1.81	60.0	169	50.65
PLACN2	95		5 [3.0]	185	1.86	60.0	170	39.01
PLACN3	93		7 [4.8]	177	1.69	59.8	170	43.66
PLACN4	94.8	0.2	5 [3.3]	181	1.76	58.6	170	41.47
PLACN5	94.5	0.5	5 [3.3]	181	1.76	57.6	169	32.91
PLACN6	93	2.0	5 [2.8]	180	1.76	54.0	168	
PLACN7	92	3.0	5 [2.4]	181	1.77	51.0	168	
PLA[a]	100			187	1.76	60.0	168	36.24
PLA1	99.8	0.2		180	1.76	58.0	168.5	46.21
PLA2	99.5	0.5		180	1.76	57.0	168.8	52.51
PLA3	98	2.0		180	1.76	54.7	169	

[a] M_w and PDI of extruded (at 190 °C) PLA are 180×10^3 (mol/g) and 1.6, respectively. [b] Value in the brackets indicates the amount of clay (inorganic part) content after burning. [c] The degrees of crystallinity.

on PLA that could have mechanical and other properties suitable for various end-use purposes. Therefore, we have attempted in this work to prepare PLA/montmorillonite nanocomposites via melt intercalation technique and then investigated the mechanical and various other properties of the nanocomposites.

Experimental Section

Materials. PLA with D content of 1.1−1.7% was supplied by Unitika Co. Ltd., Japan, and was used after being dried under vacuum at 70 °C. α,ω-Hydroxy-terminated o-PCL with weight-average molecular weight (M_w) of 2000 g/mol (L220AL) was supplied by Daicel Chemical Co. Ltd. The organically modified montmorillonite (C_{18}-mmt) used in this study as an OMLS was supplied by Nanocor Inc. and was synthesized by replacing Na^+ in montmorillonite of a cation-exchange capacity of 110 mequiv/100 g with octadecylammonium cation by ion exchange reaction.

Preparation of Nanocomposites. For nanocomposites preparation, C_{18}-mmt (powder form) and PLA (pellet form) were first dry-mixed by shaking them in a bag. The mixture was then melt-extruded by using a twin-screw extruder (S-1 KRC, Kurimoto Ltd.) operated at 190 °C to yield very light gray color strands of nanocomposites. Nanocomposites loaded with o-PCL as a compatibilizer[22] were also prepared by melt extrusion in the same manner. The compositions of the prepared nanocomposites are presented in Table 1. To investigate the effect of o-PCL on the mechanical and other properties of the nanocomposites, miscible blends of PLA and o-PCL (PLA/o-PCL) were also prepared without C_{18}-mmt (Table 1). The extruded strands were then palletized and dried under vacuum at 85 °C for 7 h to remove any water. Hereafter, the product nanocomposites were abbreviated as PLACNs.

The dried PLACNs pellets were then converted into sheets with a thickness of 0.7−2 mm by pressing with ∼1 MPa at 185 °C for 3 min. The molded sheets were then quickly quenched between glass plates and then annealed at 110 °C for 1.5 h to crystallize before being subjected to all measurements. The contents of the inorganic part in the nanocomposites were measured by burning the nanocomposite sheets at 950 °C in a furnace.

Characterization Methods. The glass transition temperature (T_g), the melting temperature (T_m), and the degree of crystallinity (χ_c) of the PLA matrices and the PLACNs were determined by a temperature-modulated differential scanning calorimeter (TMDSC) (MDSC, TA2920, TA Instruments), which was operated at a heating rate of 5 °C/min with a heating/cooling cycle of the modulation period of 60 s and the amplitude of ±0.769 °C. For the measurement of χ_c, before performing the DSC analysis, we have to subtract the extra heat absorbed by the crystallites formed during heating process from the total endothermic heat flow due to the melting of the whole crystallites. This can be done using TMDSC according to the principles and procedures described in the relevant literature.[23] By considering melting enthalpy of 100% crystalline poly(L-lactide) as 93 J/g,[24] we have estimated the value of χ_c of various PLA matrices and PLACNs. The estimated values are presented in Table 1. In the case of matrices or PLACNs prepared with o-PCL, up to 0.5 wt %, we make an approximation that melting enthalpy of PLA does not change upon o-PCL addition.

The number-average (M_n) and weight-average (M_w) molecular weights of the PLA matrix (before and after nanocomposites preparation) were determined from gel permeation chromatography (GPC; Tosoh HLC-8121) which was based on the calibration using polystyrene standards and tetrahydrofuran as a carrier solvent at 40 °C with the flow rate of 0.5 mL/min. The results of the GPC measurements are presented in Table 1. GPC data in Table 1 indicate almost no degradation of the PLA matrix after nanocomposites preparation.

WAXD experiments were performed for the C_{18}-mmt and the various PLACNs using a MXLabo diffractometer (MAC Science Co.), which has a X-ray generator of 3 kW, a graphite monochromatic, Cu Kα radiation (wavelength, $\lambda = 0.154$ nm), and operated at 40 kV/20 mA. The samples were scanned at 2°/min under the diffraction angle 2Θ in the range of 1−70°.

To investigate the nanoscale structure of the PLACNs, a transmission electron microscope (TEM) (H-7100, Hitachi Co.) was also used and operated at an accelerating voltage of 100 kV. The ultrathin sections (edge of the compress sheets) with a thickness of 100 nm were microtomed at 20 °C using a Reichert Ultracut cryoultramicrotome without staining. TEM photographs were taken from the edge of the compression-molded sheets.

Dynamic mechanical properties of the PLACNs and the corresponding matrices were measured by using a Reometrics dynamic analyzer (RDAII) in the tension−torsion mode. The temperature dependence of dynamic storage modulus (G'), loss modulus (G''), and their ratio (tan δ) were conducted at a constant frequency (ω) of 6.28 rad/s with the strain amplitude of 0.05% and in the temperature range of −20 to 160 °C with heating rate of 2 °C/min.

Melt rheological measurements were also performed on RDAII instruments with a torque transducer capable of measurements over the range of 0.2−2000 g cm. Dynamic oscillatory shear measurements were performed using a set of 25 mm diameter parallel plates with a sample thickness of 1−2 mm and in the temperature range of 170−210 °C. The strain amplitude was fixed to 5% to obtained reasonable signal intensities even at elevated temperatures or low frequency (ω) to avoid the nonlinear response. For each PLACN investigated the limits of linear viscoelasticity were determined by performing strain sweeps at a series of fixed ω's. The master curves were generated by using the principle of time−temperature superposition and shifted to a common reference temperature (T_{ref}) of 170 °C, which was chosen as the most representative of a typical processing temperature of PLA.

Results and Discussion

WAXD Patterns and TEM Observation. Direct evidence of the intercalation of the polymer chains into

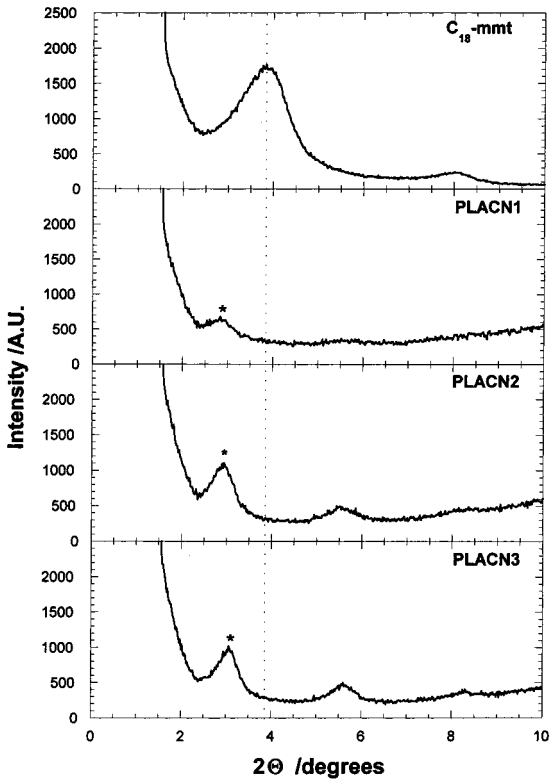

Figure 1. WAXD patterns for C_{18}-mmt and PLACNs. The dashed line indicates the location of the silicate (001) reflection of C_{18}-mmt. The asterisks indicate the (001) peak for PLACNs.

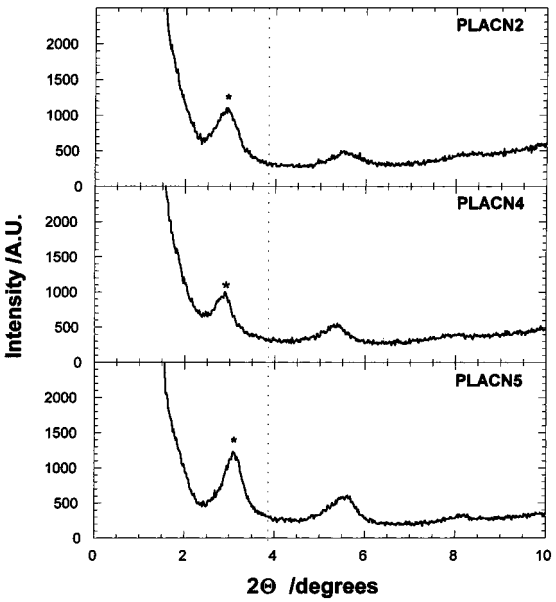

Figure 2. WAXD patterns for PLACNs with o-PCL as a compatibilizer. The dashed line indicates the location of the silicate (001) reflection of C_{18}-mmt. The asterisks indicate the (001) peak for PLACNs.

the silicate galleries is provided by the WAXD patterns in the range of $2\Theta = 1-10°$ as shown in Figures 1 and 2. The mean interlayer spacing of the (001) plane ($d_{(001)}$) for the C_{18}-mmt solid obtained by WAXD measurements is 2.31 nm ($2\Theta \cong 3.82°$) (Figure 1). In the case of PLACN1, a small peak is observed at $2\Theta \cong 2.85°$ ($\cong$ 3.10 nm), corresponding to the (001) plane of the silicate layers in the PLA matrix. With increasing clay content, this peak becomes stronger and shifted to higher diffraction angle at $2\Theta \cong 3.05°$ ($\cong$2.89 nm) for PLACN3,

Table 2. Comparison of Form Factors between PLACN2 and PLACN4 Obtained from TEM Pictures

	PLACN2	PLACN4
TEM		
d_{clay}/nm	38 ± 17.25	30 ± 12.5
L_{clay}/nm	448 ± 200	659 ± 145
L_{clay}/d_{clay}	12	22
ξ_{lay}	255 ± 137	206 ± 92
WAXD		
$d_{(001)}$/nm	3.03	2.98
$d_{clay}/d_{(001)}$	13	10

accompanied by the appearance of another peak at $2\Theta \cong 5.6°$. After calculation, it was confirmed that this peak due to (002) plane ($d_{(002)}$) of the silicate layers[25] dispersed in the PLA matrix. In each PLACN, polymer chains were intercalated in the silicate galleries, and the coherent order of the silicate layers is much higher with increasing clay content. So from the WAXD analyses, we can conclude that the ordered intercalated nanocomposite was formed in the PLACNs although the interlayer spacing increased significantly compared to that of C_{18}-mmt.

Figure 2 shows the WAXD patterns of PLACNs with o-PCL as a compatibilizer. The pattern of PLACN2 containing 3 wt % clay is displayed again as a reference. For the PLACN4 and PLACN5, the position of the (001) plane remains unchanged, but the diffraction peak of the (001) plane becomes sharper compared to that of the reference PLACN2, indicating better parallel stacking of the silicate layers upon o-PCL addition.

The internal structures of the nanocomposites in the nanometer scale were observed via TEM analysis. The structure of the nanocomposites has typically been elucidated using TEM and WAXD. TEM allows a qualitative understanding of the internal structure through direct visualization. On the other hand, WAXD offers a convenient method to determine the interlayer spacing of the clay layers in the original clay and in the intercalated polymer/clay nanocomposites. Figure 3 shows the results of TEM bright field images: (a) PLACN2 (×10 000), (b) PLACN4 (×10 000), (c) PLACN2 (×40 000), and (d) PLACN4 (×40 000), in which dark entities are the cross section of intercalated organoclay layers. For each PLACN, we observed stacked and flocculated silicate monolayers, which are randomly distributed in the PLA matrix.

In the PLACN4, individual silicate layers, which have original thickness of ~1 nm and average length of ~150 nm, connected through the edge are seen in the PLA/o-PCL matrix, and a large anisotropy of the clay layers is observed. In Table 2, we summarized the form factors obtained from TEM pictures, i.e., average length (L_{clay}), thickness (d_{clay}) of the dispersed stacked silicate layers, and the correlation length (ξ_{lay}) between them.

For PLACN2, L_{clay} and d_{clay} are in the range of 448 and 38 nm, respectively. On the other hand, PLACN4 exhibit less stacking ($d_{clay} \sim 30$ nm) of the silicate layers with L_{clay} of about 659 nm and are little orderly oriented in the matrix. From the ratio of $d_{clay}/d_{(001)}$ of each PLACN, we can estimate the number of the stacked individual silicate layers of about 13 for PLACN2 and about 10 in the case of PLACN4. Both ξ_{lay} values of the PLACNs are in the same order of magnitude compared to that of L_{clay}. Thus, nanocomposites containing a very small amount of o-PCL having terminal-hydroxy groups lead to much flocculate structure. This is due to the hydroxylated edge−edge interaction of the silicate layers.[26] Owing to the interaction between clay particles

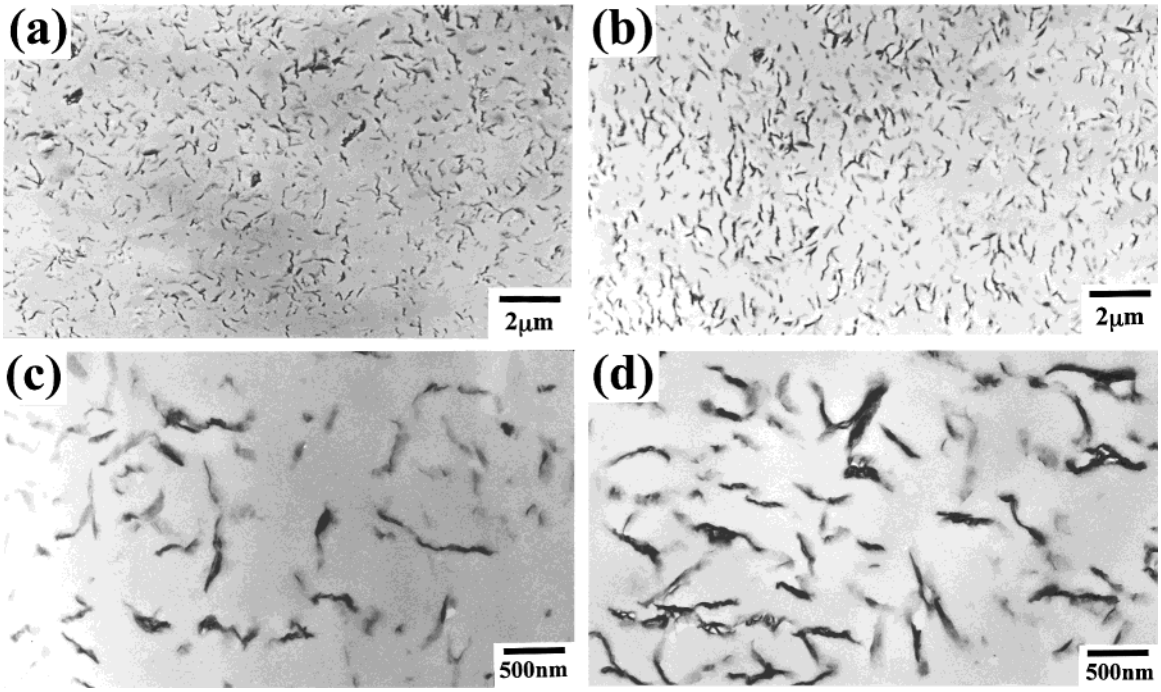

Figure 3. TEM bright field images: (a) PLACN2 (×10 000), (b) PLACN4 (×10 000), (c) PLACN2 (×40 000), and (d) PLACN4 (×40 000). The dark entities are the cross section of intercalated organoclay layers, and the bright areas are the matrices.

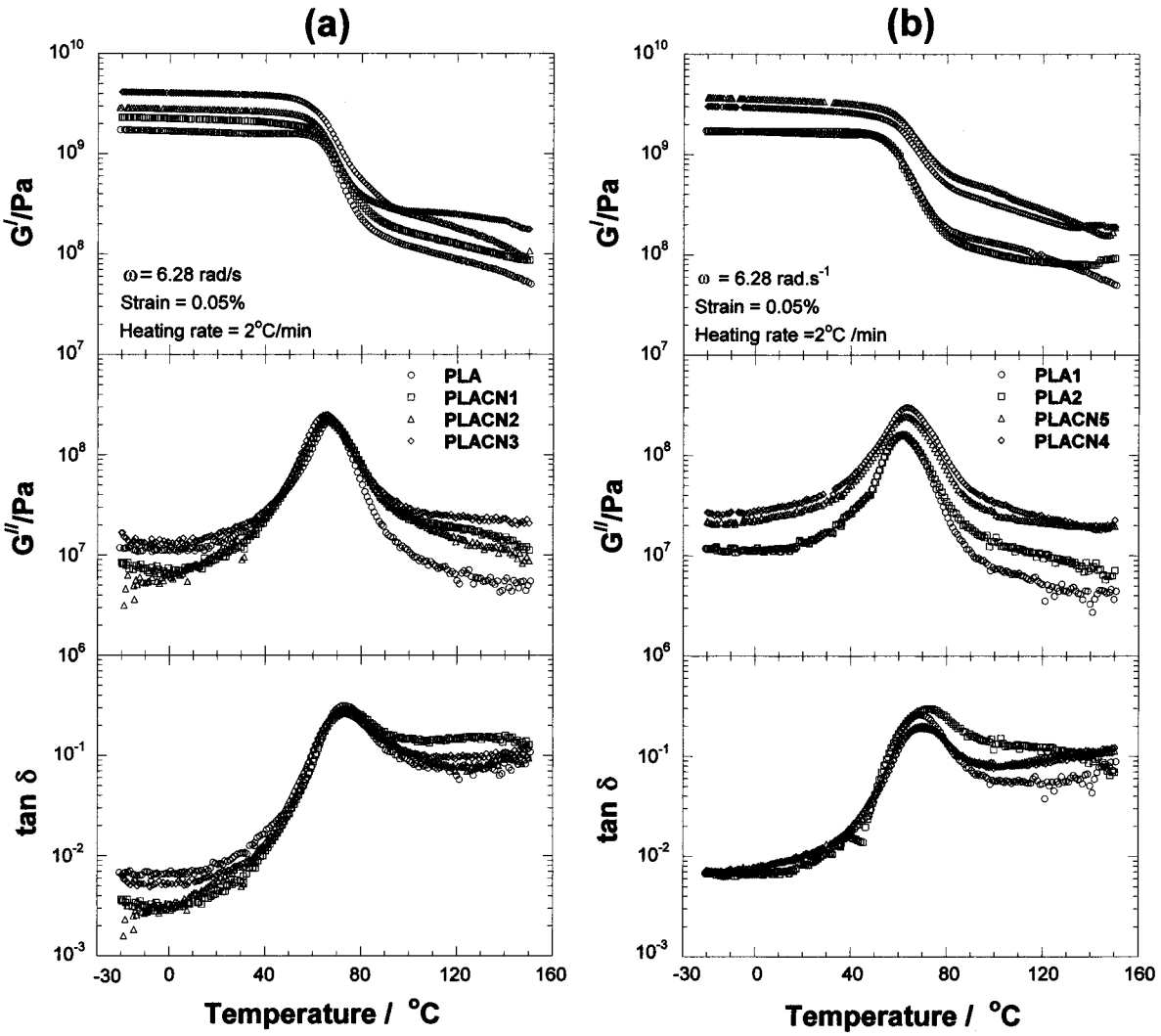

Figure 4. Temperature dependence of storage modulus (G'), loss modulus (G''), and their ratio (tan δ) for PLACNs and the corresponding matrices: (a) with out o-PCL and (b) with o-PCL.

Table 3. G' Value of All PLACNs and Corresponding Matrices without Clay at Various Temperature Range

	storage modulus, G'/GPa			
samples	−20 °C	40 °C	100 °C	145 °C
PLACN1	2.32	2.07	0.16	0.09
PLACN2	2.90	2.65	0.25	0.10
PLACN3	4.14	3.82	0.27	0.19
PLACN4	3.71	3.21	0.43	0.16
PLACN5	3.04	2.60	0.32	0.16
PLACN6	2.08	1.97	0.23	0.08
PLACN7	1.86	1.76	0.16	0.07
PLA	1.74	1.60	0.13	0.06
PLA1	1.73	1.60	0.13	0.06
PLA2	1.68	1.55	0.12	0.06
PLA3	1.67	1.62	0.12	0.06

and the PLA matrix with a small amount of o-PCL, the disk−disk interaction plays an important role in determining the stability of the clay particles and hence the enhancement of mechanical properties of such nanocomposites.

The values of χ_c calculated from the TMDSC analyses show around 33−52% for all PLACNs and the corresponding matrices (Table 1). Other interesting features are the crystallization of the intercalated PLACNs and a potential of the dispersed clay particles for nucleating agents under isothermal crystallization conditions. Such a discussion is beyond the objective of this paper, and we will report it separately.[27]

Solid-State Rheology and Enhancement of Modulus. Parts a and b of Figure 4 show the temperature dependence isochronal storage modulus (G'), loss modulus (G''), and loss tan δ of the PLA matrices and the various PLACNs, respectively. The enhancement in moduli appears in different magnitudes at various temperature ranges for all PLACNs. Below T_g, the enhancement of G' is clear in the intercalated PLACNs. At the temperature range of −20 to 50 °C, the increase in G' are 33% for PLACN1, 65% for PLACN2, and 140% for PLACN3 as compared to that of the PLA matrix (Figure 4a). Furthermore, at temperature range of 80−145 °C all the three nanocomposites exhibit much higher enhancement of G' as compared to that of PLA. This is due to both mechanical reinforcement by clay particles[28] and extended intercalation[14] at high temperature. Above T_g, when materials become soft, the reinforcement effect of the clay particles becomes prominent, due to restricted movement of the polymer chains, and hence strong enhancement of modulus appears.[2]

On the other hand, PLACN4 and PLACN5 exhibit strong enhancement of G' as compared to that of the PLACN2 with comparable clay loading and PLA/o-PCL matrices containing 0.2 and 0.5 wt % of o-PCL (abbreviated as PLA1 and PLA2, respectively) (Figure 4b). The presence of small amounts of o-PCL (up to 0.5 wt %) does not lead to a big shift and broadening of the tan δ curves. However, a large increment in G'' above T_g became clear, indicating that the large anisotropy of the dispersed clay particles due to the flocculation enhanced the loss component.

In Table 3, we summarized G' values of all PLACNs and the corresponding matrices without clay at various temperature ranges. For PLACN4, the increments in G' are 100% at 40 °C and 230% at 100 °C as compared to that of PLA and PLA1. For PLA3 with 2 wt % o-PCL as a compatibilizer, the o-PCL dose not lead to the big change of G', suggesting that o-PCL does not play the role of plasticizer.

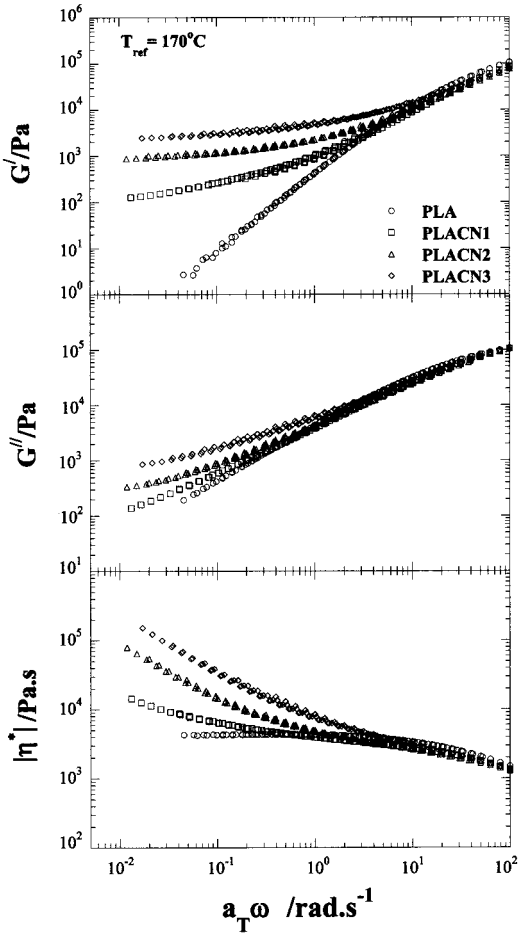

Figure 5. Reduced frequency dependence of storage modulus [$G'(\omega)$], loss modulus [$G''(\omega)$], and complex vixcosity [$|\eta^*|$] of PLACNs and PLA matrix. T_{ref} = 170 °C.

Nanocomposites with a very small amount of o-PCL (PLACN4 and PLACN5) exhibit very high enhancement of mechanical properties as compared to that of the nanocomposite with comparable clay loading (PLACN2). The essential factor governing the enhancement of mechanical properties of the nanocomposites is the aspect ratio of the dispersed clay particles.[26] From the TEM figures it is clearly indicated that, in the presence of a very small amount of o-PCL, flocculation of the dispersed clay particles took place again due to the edge−edge interaction of the clay particles. The two-dimensional aspect ratio of the dispersed clay particles L_{clay}/d_{clay} estimated from TEM observation are 22 for PLACN4 and 12 for PLACN2 (as summarized in Table 2) and hence the strong enhancement of the mechanical properties.

Melt Rheology. Figures 5 and 6 show the reduced angular frequency, $a_T\omega$ dependence of storage modulus ($G'(\omega)$), loss modulus ($G''(\omega)$), and complex viscosity ($|\eta^*|$) for all PLACNs and the corresponding matrices, respectively.

As expected, the moduli of the nanocomposites increase with increasing clay loading at all frequencies. At high frequencies, the qualitative behavior of $G'(\omega)$ and $G''(\omega)$ is essentially same and unaffected with frequencies. However, at low frequencies $G'(\omega)$ and $G''(\omega)$ increase monotonically with increasing clay content. In the low-ω region, the curves can be expressed by a power law of $G'(\omega) \propto \omega^2$ and $G''(\omega) \propto \omega$ for PLA,

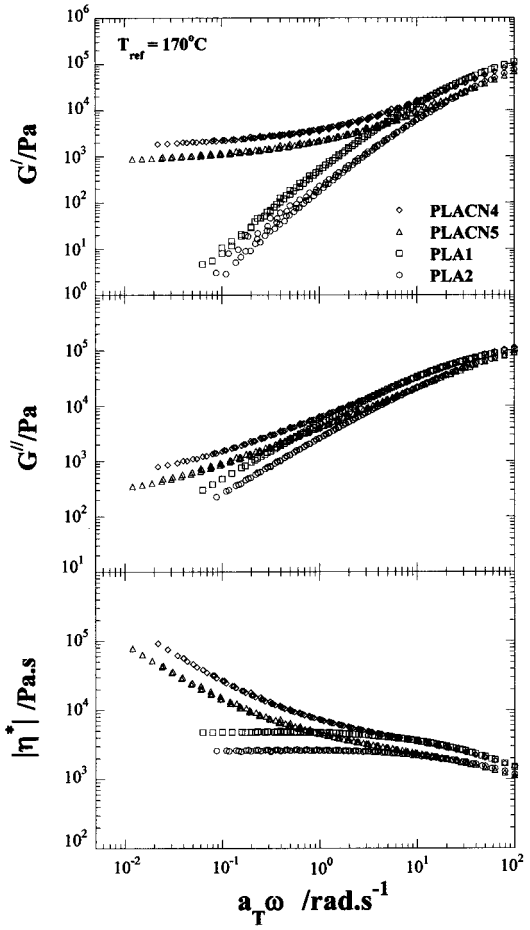

Figure 6. Reduced frequency dependence of storage modulus [$G'(\omega)$], loss modulus [$G''(\omega)$], and complex viscosity [$|\eta^*|$] of PLACNs with o-PCL and corresponding matrices without clay. T_{ref} = 170 °C.

suggesting that this is similar to those of the narrow M_W distribution homopolymer melts. On the other hand, for $a_T\omega$ < 5 rad/s, the viscoelastic response (particularly, $G'(\omega)$) for all nanocomposites displays significantly diminished frequency dependence as compared to the matrices. In fact, for all PLACNs, $G'(\omega)$ becomes nearly independent at low $a_T\omega$ and exceeds $G''(\omega)$, characteristic of materials exhibiting a pseudo-solid-like behavior.

The temperature dependence frequency shift factors (a_T, WLF type[29]) used to generate master curves shown in Figures 5 and 6 are shown in Figure 7. The near independence of the frequency shift factors on the silicate loading (Figure 7a) suggests that the temperature-dependent relaxation processes observed in the viscoelastic measurements are essentially unaffected by the presence of the silicate layers.[30]

As seen in TEM observation, ξ_{lay} values of PLACNs are smaller than that of L_{clay}, suggesting the formation of spatially linked structure of the dispersed clay particles in PLA matrix (cf. Table 2). According to this structure, the individual silicate layers are incapable of freely rotating,[31] and hence the relaxation of the structure by imposing small ω is prevented almost completely. This type of prevented relaxation due to the highly geometric constraints of the stacked silicate layers lead to the presence of the pseudo-solid-like behavior observed in PLACNs. This behavior probably corresponds to the shear-thinning tendency, which

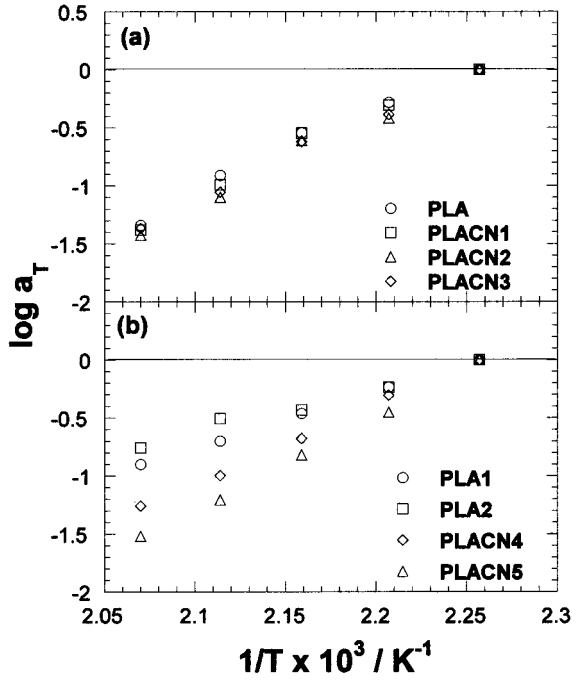

Figure 7. Frequency shift factors (a_T) as a function of temperature.

strongly appear in the viscosity curves (ω < 5 rad s^{-1}) ($|\eta^*|$ vs $a_T\omega$) of the PLACNs.

In our previous study on lyophilized smectic clay/toluene suspensions,[32] we observed shear-thinning (thixotropic) feature of the clay particles in the rapid shear flow. Such a feature strongly depended on the shear rate in the dynamic measurement because of the formation of the shear-induced alignment of the dispersed clay particles.

Conclusions

We have prepared PLA/layered silicate nanocomposites by melt extrusion of PLA and C_{18}-mmt, wherein silicate layers of the clay were intercalated and randomly distributed in the matrix. Incorporation of very small amounts of campatibilizer in the system leads to better parallel stacking of the silicate layers and also much stronger flocculation due to the hydroxylated edge−edge interaction of the silicate layers. These systems were the first successful intercalated-type PLA/layered silicate nanocomposites. The PLA/layered silicate nanocomposites exhibited remarkable improvement of materials properties in both solid and melt states compared to the matrix without clay. In our forthcoming paper,[33] we will describe the concurrent improvement of materials properties such as biodegradability, gas barrier properties, heat distortion temperature, etc., of these nanocomposites.

Acknowledgment. The present work was partially supported by the Grant-in-Aid for Academic Frontier Center under the project "Future Data Storage Materials" granted by the Ministry of Education, Science, Sports and Culture (1999−2003). We express our appreciation to the reviewers for their constructive and meticulous assessment of the manuscript.

References and Notes

(1) Messersmith, P. B.; Giannelis, E. P. *Chem. Mater.* **1994**, *6*, 1719.

(2) Usuki, A.; Kawasumi, M.; Kojima, Y.; Okada, A.; Kurauchi, T.; Kamigaito, O. *J. Mater. Res.* **1993**, *8*, 1174.
(3) LeBaron, P. C.; Wang, Z.; Pinnavaia, T. *J. Appl. Clay Sci.* **1999**, *15*, 11.
(4) Giannelis, E. P.; Krishnamoorti, R.; Manias, E. *Adv. Polym. Sci.* **1999**, *138*, 107.
(5) Alexander, M.; Dubois, P. *Mater. Sci. Eng.* **2000**, *28*, 1.
(6) Okamoto, M.; Nam, P. H.; Maiti, P.; Kotaka, T.; Hasegawa, N.; Usuki, A. *Nano Lett.* **2001**, *1*, 295.
(7) Okamoto, M.; Nam, P. H.; Maiti, P.; Kotaka, T.; Nakayama, T.; Takada, M.; Ohshima, M.; Usuki, A.; Hasegawa, N.; Okamoto, H. *Nano Lett.* **2001**, *1*, 503.
(8) Vaia, R. A.; Giannelis, E. P. *Macromolecules* **1997**, *30*, 8000 and references therein.
(9) Cao, G.; Mallouk, T. E. *J. Solid State Chem.* **1991**, *94*, 59. Pillion, J. E.; Thompson, M. E. *Chem. Mater.* **1991**, *3*, 777. Kanatzidis, M. G.; Wu, C. G.; Marcy, H. O.; deGroot, D. C.; Kannewurf, C. R. *Chem. Mater.* **1990**, *2*, 222. Mehrotra, V.; Giannelis, E. P. *Solid State Commun.* **1991**, *77*, 155; *Solid State Ionics* **1992**, *51*, 115.
(10) Aranda, P.; Ruiz-Hitzky, E. *Chem. Mater.* **1992**, *4*, 1395. Messersmith, P. B.; Stupp, S. I. *J. Mater. Res.* **1992**, *7*, 2599.
(11) Vaia, R. A.; Ishii, H.; Giannelis, E. P. *Chem. Mater.* **1993**, *5*, 1994.
(12) Hasegawa, N.; Okamoto, H.; Kato, M.; Usuki, A. *J. Appl. Polym. Sci.* **2000**, *78*, 1981.
(13) Hasegawa, N.; Okamoto, H.; Kato, M.; Tsukigase, A.; Usuki, A. *Macromol. Mater. Eng.* **2000**, *280/281*, 76.
(14) Nam, P. H.; Maiti, P.; Okamoto, M.; Kotaka, T.; Hasegawa, N.; Usuki, A. *Polymer* **2001**, *42*, 9633.
(15) Grijpma, D. W.; Pennings, A. J. *Macromol. Chem. Phys.* **1994**, *195*, 1649.
(16) Perego, G.; Cella, G. D.; Bastioli, C. *J. Appl. Polym. Sci.* **1996**, *59*, 37.
(17) Sinclair, R. G. *J. Macromol. Sci., Pure Appl. Chem.* **1996**, *A33*, 585.
(18) Tsuji, H.; Ikada, Y. *J. Appl. Polym. Sci.* **1998**, *67*, 405.
(19) Martin, O.; Averous, L. *Polymer* **2001**, *42*, 6209.
(20) Lunt, J. *Polym. Degrad. Stab.* **1998**, *59*, 145.
(21) Fang, Qi.; Hanna, M. A. *Industrials Crops Pdts.* **1999**, *10*, 47.
(22) Actually, high molecular weight PCL is immiscible with PLA, but we observed o-PCL is highly miscible with PLA (by T_g shift). Since this is a α,ω-hydroxy-terminated o-PCL, so interaction with the C_{18}-mmt is higher as compared to that of PLA, and also due to low M_w (2000 g/mol), entropic penalties is less in the case of o-PCL as compared to that of high M_w PCL. As a result, o-PCL molecules were first intercalated into the silicate galleries and then insist PLA molecules for intercalation because o-PCL is highly miscible with PLA.
(23) Wunderlich, B.; Jin, Y.; Boller, T. *Thermochim. Acta* **1994**, *238*, 277.
(24) Fischer, E. W.; Sterzel, H. J.; Wegner, G. *Kolloid Z. Z. Polym.* **1973**, *25*, 980.
(25) With respect to the (001) plane peak, the calculated value for the (002) plane peak position is $2\Theta \cong 6.08°$.
(26) Okamoto, M.; Morita, S.; Kim, Y. H.; Kotaka, T.; Tateyama, H. *Polymer* **2001**, *42*, 1201.
(27) Sinha Ray, S.; Okamoto, M.; Yamada, K.; Ueda, K., manuscript in preparation.
(28) This reinforcement is not due to the nucleation of different crystal phase in the nanocomposites because we conducted WAXD analyses up to $2\Theta = 70°$, but there is no shifting or formation of new peaks in nanocomposites.
(29) Williams, M. L.; Landel, R. F.; Ferry, J. D. *J. Am. Chem. Soc.* **1955**, *77*, 3701.
(30) Krishnamoorti, R.; Giannelis, E. P. *Macromolecules* **1997**, *30*, 4097.
(31) Ren, J.; Silva, A. S.; Krishnamoorti, R. *Macromolecules* **2000**, *33*, 3739.
(32) Okamoto, M.; Taguchi, H.; Sato, H.; Kotaka, T.; Tatayama, H. *Langmuir* **2000**, *16*, 4055.
(33) Sinha Ray, S.; Yamada, K.; Okamoto, M., manuscript in preparation.

MA011613E